ARTICLE

Effect of Atmospheric Interfering Absorption on Measurement of BTX by DOAS

Fu-min Peng[a,b], Pin-hua Xie[a*], Hai-yang Li[c], Ying-hua Zhang[a], Jun-de Wang[c], Wen-qing Liu[a]

a. Key Laboratory of Environmental Optical and Technology, Anhui Institute of Optics and Fine Mechanics, Chinese Academy of Sciences, Hefei 230031, China
b. College of Chemistry and Chemical Engineering, Anhui University, Hefei 230039, China
c. Dalian Institute of Chemical Physics, Chinese Academy of Sciences, Dalian 116023, China

(Dated: Received on July 26, 2007; Accepted on December 19, 2007)

It was reported on the elimination of interfering absorption of BTX. the absorption of O_2 includes different absorption bands, which change differently when the partial pressure of oxygen is varied. These cause the nonlinear absorption of O_2 and the observed band shape to vary with the column density of O_2. The absorption ratios of molecular absorption in each of the Herzberg bands and dimer absorptions, as well as the contribution to the correction error of molecular absorption, are studied based on the characteristic of these absorption bands. The optimized way to eliminate the interfering absorption is obtained in the end and the effectiveness of using interpolation proposed by Volkamer *et al.* to remove O_2 absorption is proved again. As to O_3 and SO_2, the effect of the thermal effect of characteristic spectra on the elimination error of their absorption is studied. Solutions to these problems are discussed and demonstrated together with methods to optimize the interpolation of spectra. As a sample application, differential optical absorption spectroscopy (DOAS) measurements of BTX are carried out. Results show a low detection limit and the good correlation with point instruments are achieved. All these prove the feasibility of using spectral interpolation to improve the accuracy of DOAS measurements of aromatic hydrocarbons for practical purposes.

Key words: Differential optical absorption spectroscopy, BTX, Herzberg band, O_2 dimer

I. INTRODUCTION

The importance of the contribution of monoaromatic hydrocarbons (MAHCs) to problems of urban air pollution has been known for some time [1-4]. Benzene, toluene and xylenes, commonly called BTX, are the most abundant among MAHCs [4-6]. The major sources of BTX in the atmosphere are emissions from motor vehicles [7,8] and solvent use [9] with minor contributions from biomass burning and biogenic emissions [10,11]. Besides their carcinogenic and mutagenic effects on living organisms and human health, the main importance of BTX with regard to air pollution is their role as precursors for the formation of photooxidants [4-6] and secondary organic aerosols [1]. The contribution of MAHCs to the ozone formation in Europe has reached up to 40% [2], which suggests MAHCs are the most important class of VOCs (volatile organic compounds) in photochemical ozone formation.

In order to comply with new regulations and scan pollutants in a large area giving instantaneous measurements of background pollution, the selective and continuous measurement techniques for these species in ambient air are needed. The mixing ratios of BTX are commonly determined by gas chromatography (GC) coupled with a flame ionization detector (FID) or mass spectrometer (MS). Application of long-path DOAS (differential optical absorption spectroscopy) [12] is one good alternative to BTX measurement by GC [13,14], since it allows direct detection without sampling loss and does not require pre/post-processing for data acquisition. It also allows real-time measurement of several species with high time resolution and sensitivity. In addition, the isomer of xylene and trimethyl-benzene that could not be separated by traditional GC methods can be identified and quantified individually by DOAS. However, the application of the DOAS technique for this group of compounds is not without problems, because of spectral interference between different aromatic as well as ozone, oxygen, and sulfur dioxide. This work focuses on the nature and source of interference of BTX measurements by DOAS and the optimum interference-elimination methods are discussed base on the characteristics of interfering absorptions.

II. THEORIES AND INSTRUMENTS

The analysis of DOAS spectra is based on the Lambert-Beer's law [14]:

$$D = \ln \frac{I_0(\lambda)}{I(\lambda)} = L\left[\sum_{i=1}^{n} \sigma_i(\lambda) C_i + \mu_{\mathrm{R}}(\lambda) + \mu_{\mathrm{M}}(\lambda)\right] \quad (1)$$

A differential optical density D is defined in Eq.(1), λ is wavelength, $I_0(\lambda)$ is intensity of the light source, $I(\lambda)$

*Author to whom correspondence should be addressed. E-mail: pengfm@dicp.ac.cn

is light intensity after pass through the atmosphere, $\mu_R(\lambda)$ is Rayleigh-scattering coefficient, $\mu_M(\lambda)$ is Mie-scattering coefficient, $\sigma_i(\lambda)$ is differential absorption cross section of absorber i, C_i is the concentration of absorber i, L is total light path length, n is the number of absorbers. Numerical filters and special algorithms remove broadband variation of the cross section as well as the wavelength dependency of the measured spectra due to Rayleigh- and Mie-scattering and the lamp. The species concentration can then be calculated according to Eq.(2):

$$C_i = \frac{D_i(\lambda)}{\sigma_i'(\lambda)L} \tag{2}$$

In theory, after removing the absorptions of different species, the residual is constituted mainly by short noise. Usually, the minimum detectable optical density is indicated as the difference between the maximum and minimum values in the residual spectrum.

DOAS system: a Cassegrain telescope with a high pressure Xenon short-arc lamp (150 W, Osram, Germany) as the light source; thirteen retro reflectors, a spectrometer (Acton500, focal length is 500 mm, grating are 1800, 1200, and 600 L/mm blazed at 300, 300, and 500 nm, respectively), a fiber bundle, 1024 pixels photo diode array (PDA) (Hoffman Messtechnik GmbH, Germany) kept at −30 °C. The data produced by the detector was digitized by a 16-bit analog-to-digital converter (ADC) and then transmitted to the Hoffman controller. After being processed, the signals were transferred to the computer by RS232. The measurement of three different types of spectra is required: the atmospheric spectra, a lamp spectra and spectra of the background light. The DOAS spectra evaluation algorithm is well described in Ref.[14].

III. ANALYSIS OF INTERFERING ABSORPTION

A. Interfering absorption of O_2

In the UV spectral region below 300 nm O_2 molecules show weak absorption due to electronic excitation in the Herzberg I ($A^3\Sigma_u^+ \leftarrow X^3\Sigma_g^-$), Herzberg II ($C^1\Sigma_u^- \leftarrow X^3\Sigma_g^-$), and Herzberg III ($A'^3\Delta_u \leftarrow X^3\Sigma_g^-$) transitions (shown in Fig.1). At the same time, Herzberg III ($A'^3\Delta_u \leftarrow X^3\Sigma_g^-$) give rise to additional diffuse absorption bands due to O_2-dimers [15]. All four band-systems strongly overlap, extending from the joint dissociation limit of O_2 at 242.9 nm towards longer wavelengths with the absorption becoming negligible above 287 nm. Regarding the transparency of the ground level atmosphere in the UV (below 300 nm), Ditchburn and Young concluded that attenuation by O_2 in the Herzberg systems was comparable to extinction by tropospheric ozone and consequently has to be taken into account in transparency calculations [16]. O_2 is the most important absorber in the UV, and its absorption

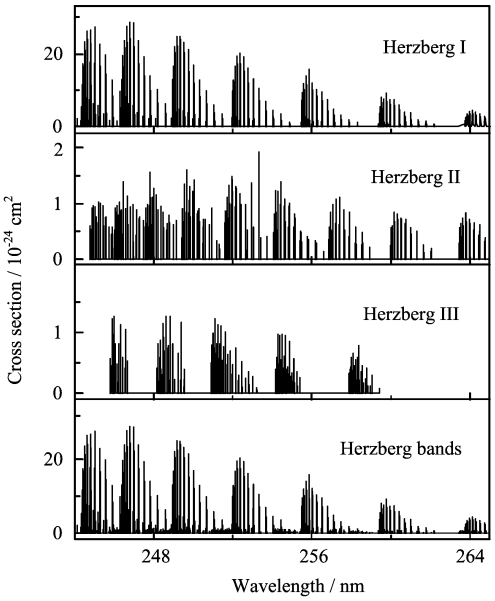

FIG. 1 The cross section spectra of the Herzberg bands system of O_2 [22-24].

is constituted mainly by Herzberg band-systems and O_2-dimers' absorption-bands. In 1915, Warburg first mentioned a quadratic pressure dependence of the absorption of gaseous oxygen [18] and Wulf first ascribed this behavior to the formation of oxygen-dimers [19]. At a pressure of about 400 kPa of pure O_2, dimers' absorption begins to dominate O_2-absorption [17]. The important dimers in the atmosphere are O_2-O_2 and O_2-N_2, overlapped with Herzberg band-systems. In any case, dimer-formation forces the cross section to increase linearly with pressure, which for dimer-absorption in the Herzberg band's wavelength range was observed in pure oxygen gas [20,21] as well as in mixtures with other gases, e.g. nitrogen, argon [17,18]. Moreover, the O_2-N_2 complex is only half as strong an absorber as the O_2-O_2 complex, leading to a predominant fraction (66%) of the dimer-absorption to be due to O_2-N_2 complexes under atmospheric conditions [17].

The interfering absorption of O_2 poses several problems for the measurements of BTX by DOAS, which were well researched by Volkamer *et al.* [5]. (i) The Herzberg bands consist of a series of narrow ro-vibronic lines with a width of the order of 1 pm. In order to fully resolve these lines a spectral resolution well below 1 pm (Γ: indicated as full width at half maximum, FWHM) would be required. Spectral resolution used in DOAS system is usually much larger than 1 pm, so the individual lines can not be separated and the apparent optical density (OD) will not increase linearly with the O_2 concentration (or L). As a consequence, the shape of the spectral features will depend on the O_2 column density. These effects of unresolved bands generally limit the linear range of DOAS measurements [17], but are of special importance for the correction of

DOI:10.1088/1674-0068/21/03/202-210

the Herzberg bands since at atmospheric path lengths of a few hundred meters, the stronger lines of the Herzberg I bands ($\sigma \leq 1.6\times10^{-22}$ cm^2) become saturated. σ of Herzberg absorption-bands depends on λ, and great difference exists in the intensity of absorption lines, so the nonlinearity effect of O_2 absorption spectrum is different from this wavelength range to the other. A single reference spectrum taken at a different column density then cannot be scaled linearly to eliminate both "weak" and "strong" absorptions in a measured spectrum at the same time. As a consequence, residual structures remain.

(ii) When the O_2 partial pressure is changed, the different absorption-bands of O_2 scale differently. Namely the Herzberg bands scale in a way different from that of dimer-absorptions and even three Herzberg bands and the absorption of two dimers (O_2-O_2 and O_2-N_2) scale in a way different from each other. In addition, all these absorption-bands overlap with each other and can not be separated, so it is impossible to correct these absorption-bands in a measured spectrum separately. The relative strength absorption of O_2-O_2 and O_2-N_2 scales differently from the O_2 partial pressure. Even though this effect can reduce the change of the ratio of molecular absorption in the Herzberg bands and dimer-absorptions, it needs to be accounted for, if the DOAS is used to measure BTX in the atmosphere.

(iii) The absorptions of O_2 and BTX overlap with each other, and the absorption features of O_2 may influence the apparent absorption features of BTX at long path lengths if spectral features are measured at "low" resolution. Hence, further residual structures may result from an incomplete correction of the absorption features of the atmospheric absorber [21].

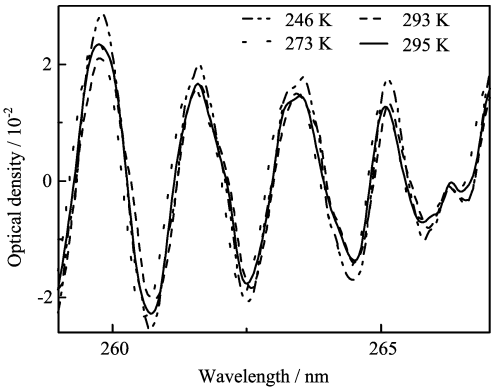

FIG. 2 The differential absorption spectra of O_3 at different temperatures (Γ=0.15 nm).

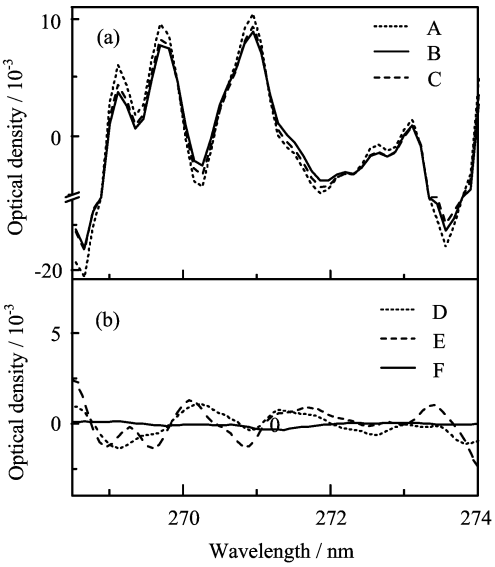

FIG. 3 The SO_2 differential absorption spectra at different temperatures (Γ=0.15 nm). (a) A: 243 K, B: 273 K, C: 293 K. (b) The residual structures after fitting A to B (D), C to B (E), and A and C (simultaneously) to B (F) corresponding to optical densities of 0.9%, 0.8%, and 0.009%, respectively.

B. Interfering absorptions of O_3 and SO_2

The absorptions of BTX overlap with those of O_3 and SO_2 besides O_2 (shown in Fig.2 and Fig.3). Though the intensities of two gases' differential cross sections are less than that of most BTX, their concentrations are ten times or even one hundred times higher than BTX, and their differential absorption ODs in the atmospheric spectra are much higher than BTX. Especially in China, SO_2 concentration is usually high in most places. As a consequence, the slight elimination error of O_3 and SO_2, which is negligible for the quantification of O_3 and SO_2 by DOAS, will introduce additional features to the residual and interfere the retrieval of BTX concentrations.

IV. EFFECT OF ABSORPTION ON MEASUREMENT RESULTS

A. Interfering evaluation of O_2 absorption

To characterize the magnitude of the O_2 interference with DOAS measurements of BTX, the signal of benzene in a measured spectrum can be compared to that of the nearby O_2 band at 259 nm. When L=682 m and Γ=0.15 nm, O_2 bands in atmospheric spectra have an OD of $\sim$0.06. Assuming a mixing ratio for benzene of 1.5×10^{-9} (a typical level in the urban air), benzene will have an OD of 3.3×10^{-3}, 5.5% of O_2 absorption. That means that the O_2 absorption will dominate the measured spectrum and even when the elimination error of O_2 absorption is kept as low as 1%, it will be difficult to accurately detect benzene for most of time in urban sites. Fortunately, most BTX show their strongest absorption bands towards longer wavelengths, where the O_2 absorption is weaker (Fig.4) [5], but still the O_2 absorption bands are likely to be stronger than the aromatic absorption, since most aromatics are present at lower concentrations than benzene.

DOI:10.1088/1674-0068/21/03/202-210

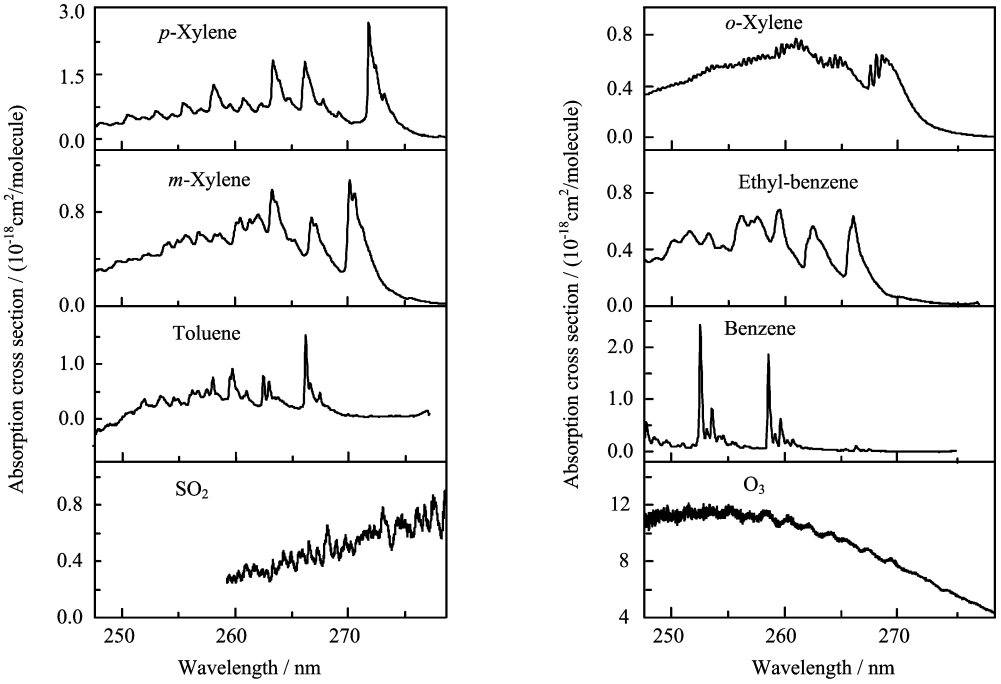

FIG. 4 The absorption cross sections of BTX [5].

B. Interfering evaluation of O_3 and SO_2 absorption

The elimination error of O_3 and SO_2 absorption mainly originates from the temperature effect of absorption cross section. However the atmospheric temperature changes inevitably and periodically. Taking a mixing ratio of 6×10^{-8} (a typical level in the urban air) as an example, the differential absorption spectra of O_3 at different temperatures are shown in Fig.2 (L=682 m, Γ=0.15 nm) and OD increases with the decrease of temperature. In order to study if the changes of O_3 differential absorption spectra at different wavelength range are synchronous, the differences of relative intensity are calculated at different wavelength, as shown in Fig.5. With the increase of temperature, the change magnitude of differential spectra depends on λ. If a single reference spectrum taken at a different temperature then cannot be scaled linearly to eliminate both, "weak" and "strong" absorptions in a measured spectrum at the same time. As shown in Fig.2, the differential absorption OD of O_3 (280 K) at 259 nm is ∼4.3%, thirteen times higher than that of benzene detected at the same time. When a reference spectrum taken at 273 or 295 K is used to fit this spectrum, 0.8% and 1.0% residual noise will remain respectively, both of which are much larger than the differential absorption OD of benzene (1.5×10^{-9}). Though O_3 absorption is weaker towards longer wavelengths, it is still likely to be stronger than the BTX absorption.

In the same way, as shown in Fig.3 and Fig.5, the absorption cross section of SO_2 also suffers from temperature effect and the change magnitude of differential spectra depends on λ with the increase of temperature. SO_2 is usually higher in China and taking a mixing ratio of 10^{-7} (a typical level in the urban air) as an example, the differential absorption OD of SO_2 (280 K) at ∼270 nm is ∼3.0% (273 K, L=682 m, Γ=0.15 nm), much higher than that of BTX in this wavelength range. As shown in Fig.3 [5], the difference between the SO_2 differential spectra at different temperatures can lead to 0.8% and 1.0% additional residual respectively, which are much larger than the differential absorption ODs. The SO_2 absorption in the detected atmospheric spectra is usually much higher than BTX, so the slight change of absorption feature will make the retrieval of BTX difficult.

V. ELIMINATION OF THE INTERFERENCES

The magnitude of the O_2, SO_2, and O_3 interference with DOAS measurements of BTX is all determined by their elimination error, so the accurate elimination of interfering absorptions is critical to DOAS measurements of BTX.

A. Elimination of O_2 interference

Axelsson *et al.* and Trost used a "zero" reference spectrum taken in "clean" air to correct O_2 absorption [26,27]. However, this method will introduce an unknown negative offset for all species present in the "zero" spectrum, as this spectrum is subtracted from each measured spectrum. Volkamer *et al.* proposed a

DOI:10.1088/1674-0068/21/03/202-210

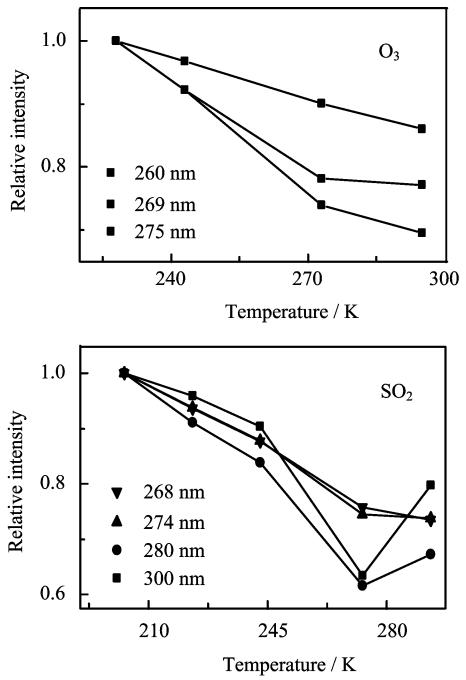

FIG. 5 The relative intensity of differential absorption spectra of O_3 and SO_2 at different temperatures.

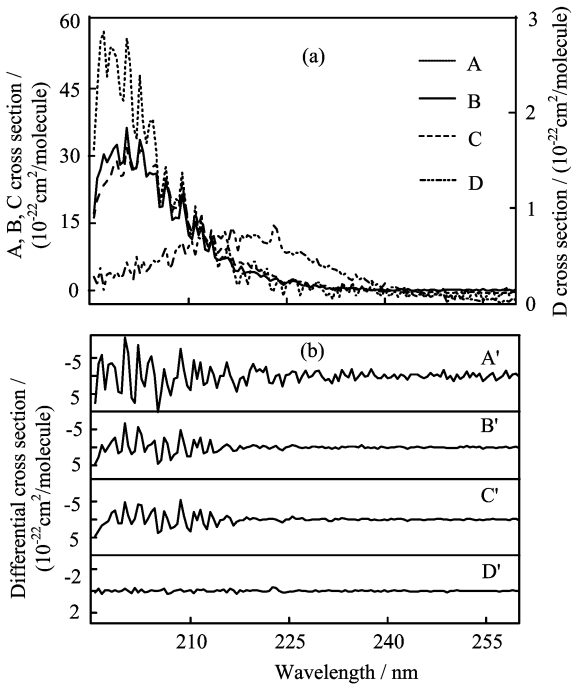

FIG. 6 The O_2 absorption cross section at different temperatures and pressures. (a) A. 1073 K, 100 kPa; B. 1073 K, 400 kPa; C. 1073 K, 600 kPa; D. 293 K, 600 kPa. (b) A′, B′, C′, and D′: the resulting spectra of A, B, C, and D respectively after being high filtered.

solution to this problem–using interpolation to remove O_2 absorption and proved it [5]. Here we used more details to prove the effectiveness of this method.

$$O_2 + O_2(N_2) \rightleftharpoons O_2\text{-}O_2(O_2\text{-}N_2)$$

As said above, absorption features of O_2-O_2 and O_2-N_2 overlapped with Herzberg bands should be separated first, in order to remove O_2 absorption from the measured spectrum. As shown in Eq.(3), the formation of O_2-O_2 depends on the pressure, which causes a quadratic pressure dependence of the absorption of gaseous oxygen and a linear pressure dependence of the absorption of dimer [21,28]. With regard to the dimer's nature, the classification of oxygen dimers under atmospheric conditions as mixtures of metastable Van der Waals dimers, metastable form and colliding pairs are most possible. Only bound Van der Waals dimers should exhibit structured absorption features, metastable form and colliding pairs would result in broadened absorptions [29].

By adjusting a spectrum taken in different oxygen/nitrogen ratios, band positions and bandwidths of the dimer absorption below 267 nm could be determined. These spectra cannot be used as dimer reference spectra since residual structures due to the unresolved molecular absorption (Fig.6) superimpose with the dimer absorption. Figure 6(a) shows the absorption cross section of O_2 at different pressures and temperatures [30]. It is clear that the band positions and bandwidths of the dimer absorption depend on pressures and temperatures, and the bandwidths of the dimer absorption are much wider than the BTX absorption. As shown in Fig.6(b), by the application of an optimized Savitzky Golay high pass filter [31,32], the wide band absorption can be almost eliminated. Seen from filtered spectra A′, B′, and C′, the wide absorption of oxygen dimers that exist in O_2 absorption can be eliminated in the same way and the narrow absorption of oxygen remains. The narrow absorption of oxygen is less dependent on pressure, so A′, B′, and C′ have similar absorption features. Due to the great difference of measurement conditions, the difference between the absorption features of D′ and A′, B′ or C′ is relatively large.

After the elimination of the absorption of O_2 dimers, the overlapped Herzberg bands need to be separated in order to eliminate the oxygen absorption present in the atmospheric spectra. As shown in Table I, the absolute oscillator strengths (f) for these three systems are 8.49×10^{-10}, 0.44×10^{-10}, and 0.51×10^{-10} [23-25] and the Herzberg I transition be more than one order of magnitude stronger than the Herzberg II and Herzberg III systems, it also can be seen from Fig.1 that the strong lines of the Herzberg I band dominate the spectrum and the absorption features of the Herzberg II and Herzberg III systems can be negligible. Therefore, the absorption features of Herzberg I determine the nonlinearity absorption features of Herzberg bands systems. In addition, as seen from the line intensity of Herzberg

DOI:10.1088/1674-0068/21/03/202-210

TABLE I Spectroscopic properties of the Herzberg transitions

Syatem	Spectroscopic notation	Selection rule violated	f	Relative strength
Herzberg I	$A^3\Sigma_u^+ \leftarrow X^3\Sigma_g^-$	$\Sigma^+ \not\leftrightarrow \Sigma^-$	$\approx 8.49\times10^{-10}$ [22]	19.3
Herzberg II	$C^1\Sigma_u^- \leftarrow X^3\Sigma_g^-$	$\Delta\Sigma \neq 0$	$\approx 0.44\times10^{-10}$ [23]	1.0
Herzberg III	$A'^3\Delta_u \leftarrow X^3\Sigma_g^-$	$\Delta\Delta = 0,\pm1$	$\approx 0.51\times10^{-10}$ [24]	1.2

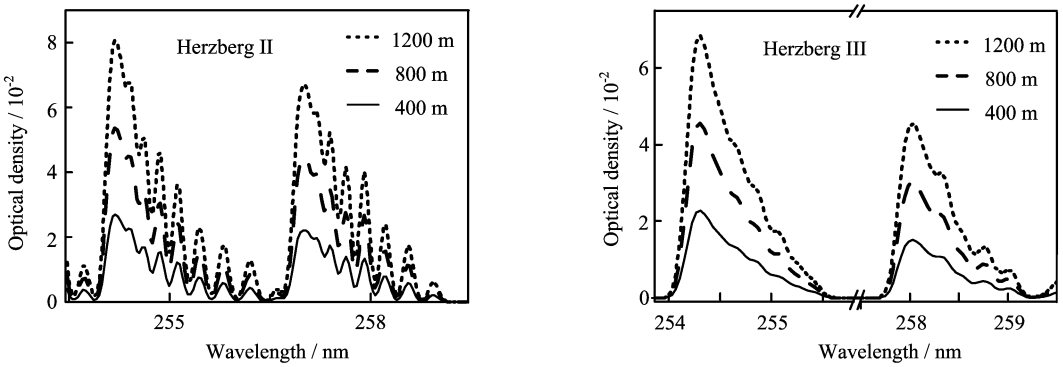

FIG. 7 Oxygen reference spectrum of the Herzberg II and III (Γ=0.15 nm).

II and III, very few lines can become saturated at atmospheric path lengths of a few hundred meters.

As shown in Fig.7, cross sections for Herzberg II and Herzberg III are calculated using the integrated absorption cross sections [24,25]. The resulting cross section spectrum is used to calculate absorption spectra for oxygen at three column densities, which are chosen to differ by a constant value and are equivalent to a ground level path length in the atmosphere of 400, 800, and 1200 m. Subsequently, these spectra are convoluted with a Gaussian-shape instrument function (Γ=0.15 nm) in order to adjust them to a resolution comparable to atmospheric DOAS measurements. When L=800 m, the differential absorption ODs of Herzberg II and III are 3.8×10^{-2} (260 nm) and 2.5×10^{-2} (258 nm) respectively. The change of L has little effect on the absorption features and when the differential spectra at different column densities are used to fit each other, the residual structure is in a level less than 10^{-6}. So this slight difference has almost no effect on the absorption feature changes of O_2.

After removing the interference of Herzberg II and Herzberg III absorption, the last step is the accurate elimination of nonlinearity absorption of Herzberg I absorption. In the same way as said above, absorption spectra of Herzberg I at path lengths of 400, 800, and 1200 m are calculated (Γ=0.15 nm), as shown in Fig.8. The individual ro-vibronic transitions are not resolved and appear as Q-branches in the spectrum. The nonlinearity of the increasing absorption features can already be seen in Fig.8, as the vertical spacing between the spectra A and B is larger than that between the spectra B and C. The change in the relative strength of the bands is clearly visible. This becomes more obvious when seen in the residual structures shown in Fig.8(d). When A or C absorption spectrum is used to correct for the absorption features of B spectrum, the residual remains at several percent. Therefore, it is impossible to correct for the absorption features of O_2 just using one O_2 reference spectrum detected at different column density. When A and C are used simultaneously to correct for B spectrum, the remained residual noise can be reduced to less than 10^{-4}. This finding provides the basis for the development of a fairly successful procedure for oxygen reference spectra interpolation.

B. Elimination of SO_2 and O_3 interference

The temperature effect on O_3 absorption features is relatively large. In order to characterize the magnitude of temperature effect on the change of absorption features, the absorption cross sections of O_3 at different temperatures are used to calculate absorption spectra with 6×10^{-8} concentration at a light path of 682 m. Subsequently, these spectra are convoluted with a Gaussian-shape instrument function (Γ=0.15 nm) and are used to calculated differential absorption spectra. The fitting errors between these spectra are indicated as the remaining noise after using one spectrum to correct for another. Using one differential absorption spectrum at different temperatures separately or simultaneously with the spectrum at 295 K to correct for the differential absorption spectrum x (x was the O_3 absorption spectrum at 280 K), the fitting results are shown in Table II. It can be seen that when only one spectrum is used, as the temperature of used spectrum become closer and closer to 280 K, the fitting error becomes less and less. However, it is still at the level of 10^{-3}; but when two

DOI:10.1088/1674-0068/21/03/202-210

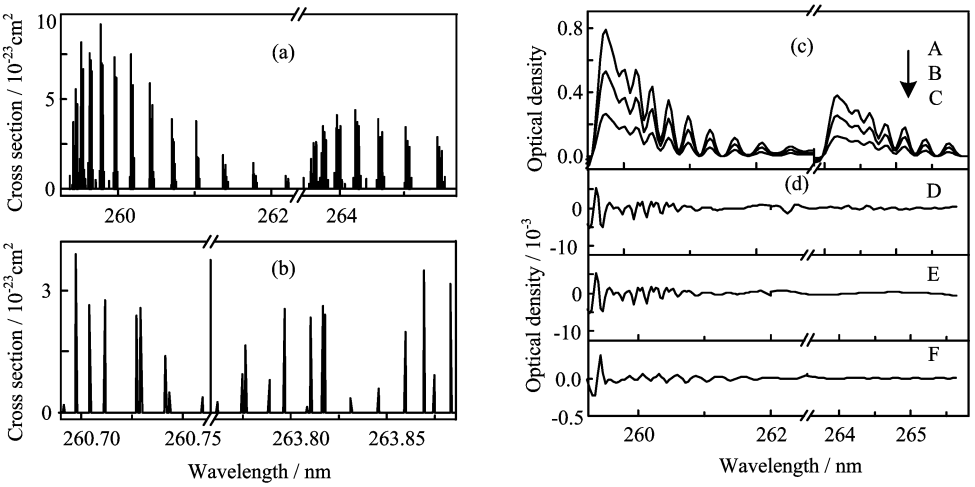

FIG. 8 The 4-0 and 5-0 vibronic band of the Herzberg I band system of O_2 [23]. (a) High resolution absorption cross section. (b) Two part of cross section shown in layer (a). (c) The shown spectra correspond to L=400 m (A), 800 m (B), and 1200 m (C) (Γ=0.15 nm). (d) The remaining residual structures (D, E, and F) after B are fitted by A and C separately and simultaneously.

TABLE II The difference among the differential absorption spectra at different temperatures

Temperature/K		228	230	246	273	293	295
Fitting error/0.1%	1	9.25	7.18	5.01	2.45	3.08	3.29
	2	0.74	0.67	0.31	0.07	–	–

1: The fitting error of differential absorption spectra at different temperature to x (the O_3 absorption spectrum at 280 K).
2: The fitting error of differential absorption spectra at different temperature and differential absorption spectra at 295 K to x (the O_3 absorption spectrum at 280 K); wavelength range: 255-270 nm.

spectra with different temperatures are used, the fitting error can be reduced to the level of 10^{-4}-10^{-5}, much less than the detection limit of benzene. That means that when two spectra with the temperature closer to the detected spectrum are used, the fitting error can be reduced as small as possible.

As shown in Fig.3, the fitting error resulting from the temperature effect of SO_2 can be reduced to the level of 10^{-5}, much less than the detection limit OD of xylene.

VI. MEASUREMENT RESULTS AND CONCLUSION

In July of 2007, long time continuous monitoring of BTX was carried out at Environmental Monitoring Department of Guangzhou with a time resolution of about 3-8 min. A ventilative measurement site with some small emission source distributed equally around was selected. The results are shown in Fig.9 and are compared with the detected results of gas chromatography (GC) (shown in Fig.10). It can be seen from the results that the same trend of BTX diurnal variation can be obtained from these two methods with high correlation. Correlation coefficient for toluene is 0.9209, benzene 0.8864, and *m*&*p*-xylene 0.8118. Only the BTX absolute concentrations of two methods have some difference. Certainly this difference may come from different principles: line measurements are used in DOAS where measurements are performed along an optical path, and point measurements are used in GC where measurements are carried out by taking samples at one spot. The detection limits of BTX are calculated based on the residual noise (10^{-3}) remaining after removing

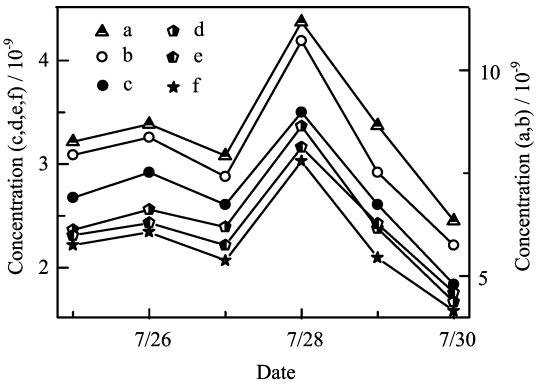

FIG. 9 The diurnal fluctuation of BTX concentration in the atmosphere. a, c and e: The results of DOAS. b, d and f: The results of GC. a and b: Toluene; c and d: Benzene; e and f: *m*&*p*-xylene.

DOI:10.1088/1674-0068/21/03/202-210

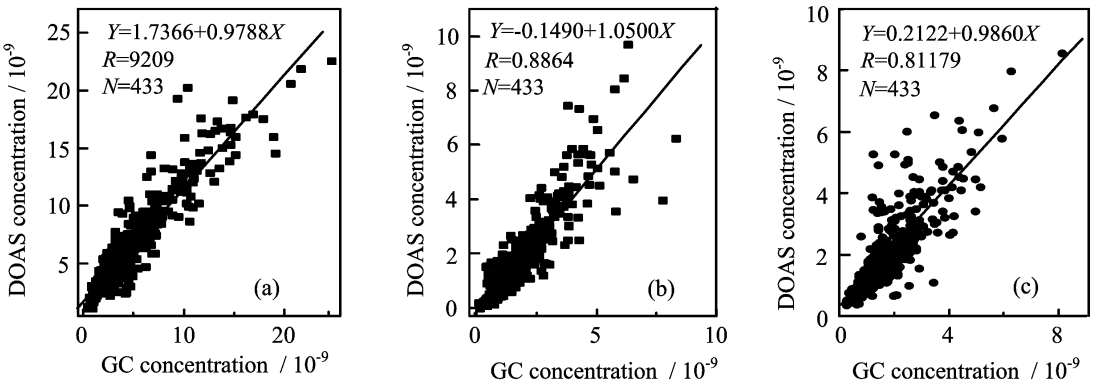

FIG. 10 The correlation between the results of DOAS and GC. (a) Toluene. (b) Benzene. (c) *m*&*p*-xylene

TABLE III The detection limit of BTX

Aromatic	Formula	Molecule weight	CAS	Detection limit/10^{-12}
Benzene	C_6H_6	78	71-43-2	280
Toluene	C_7H_8	92	108-88-3	380
o-Xylene	C_8H_{10}	106	95-47-6	200
m-Xylene	C_8H_{10}	106	108-38-3	504
p-Xylene	C_8H_{10}	106	106-42-3	1500

the absorptions of all species, as shown in Table III. By the use of the method explained above, the remaining residual noise is almost all short noise. It can be seen that the optimized application of spectral interpolation can be successfully used to remove the interfering absorption of O_2, SO_2 and O_3 and achieve the accurate measurement of BTX. This method has not only a strong theoretical foundation, but also practical feasibility.

Featuring excellent response characteristics and detection sensitivity and with much lower operational cost, differential optical absorption spectroscopy (DOAS) can be a powerful tool to trace concentration variation of BTX (the main aromatic compounds in the atmosphere). This work focuses on the elimination of interfering absorption of BTX: the absorption of O_2 includes different absorption bands, which change differently when the partial pressure of oxygen is varied. Namely the Herzberg bands change in the way different from that of dimer absorption and even three Herzberg bands and the absorption of two dimers (O_2-O_2 and O_2-N_2) change in ways different from each other. These cause the nonlinear absorption of O_2 and the observed band shape to vary with the column density of O_2. The absorption ratios of molecular absorption in each of the Herzberg bands and dimer absorptions, as well as the contribution to the correction error of molecular absorption, were studied based on the characteristic of these absorption bands. The optimized way to eliminate the interfering absorption is obtained in the end and the effectiveness of using interpolation proposed by Volkamer *et al.* to remove O_2 absorption is proved again. As to O_3 and SO_2, the effect of the thermal effect of characteristic spectra on the elimination error of their absorption is studied. Solutions to these problems are discussed and demonstrated together with methods to optimize the interpolation of spectra. As a sample application, DOAS measurements of BTX were carried out and a low detection limit and good correlation with point instruments was achieved. These evidences prove the feasibility of the methods.

VII. ACKNOWLEDGMENT

This work was supported by the National Natural Science Foundation of China (No.20273066).

[1] J. R. Odum, T. P. W. Jungkamp, R. J. Griffin, R. C. Flagan, and J. H. Seinfeld, Science **276**, 96 (1997).
[2] R. G. Derwent, M. E. Jenkin, and S. M. Saunders, Atmos. Environ. **30**, 181 (1996).
[3] R. Atkinson and S. M. Aschmann, Int. J. Chem. Kinet. **26**, 929 (1994).
[4] T. Etzkorn, B. Klotz, S. Sörensen, I. V. Patroescu, I. Barnes, K. H. Becker, and U. Platt, Atmos. Environ. **33**, 525 (1999).
[5] R. Volkamer, T. Etzkorn, A. Geyer, and U. Platt, Atmospheric Environment **32**, 3721(1998).
[6] K. Kourtidis, I. Ziomass, C. Zerefos, E. Kosmidis, P. Symeonidis, E. Christophilopoulos, S. Karathanassis, and A. Mploutsos, Atmos. Environ. **36**, 5355 (2002).
[7] D. Brocco, R. Fratarcangeli, L. Lepore, M. Petricca, I. Ventrone, Atmos. Environ. **31**, 557 (1997).
[8] K. Kim, Enviro. Engineering Sci. **21**, 181 (2004).
[9] S. D. Piccot, J. J. Watson, and J. W. Jones, J. Geophys. Res. **97**, 9897 (1992).
[10] K. Nikolau, P. Masclet, and G. Mouvier, Sci. Total Enviro. **32**, 103 (1984).
[11] F. Fehsenfeld, J. Calvert, R. Fall, P. Goldan, A. B. Guenthner, C. N. Hewitt, B. Lamb, S. Liu, M. Trainer,

DOI:10.1088/1674-0068/21/03/202-210

H. Westberg, and P. Zimmerman, Global Biogeochem. Cycles **6**, 389 (1992).
[12] C. Lee, Y. J. Choi, J. S. Jung, J. S. Leea, K. H. Kimb, and Y. J. Kima, Atmos. Environ. **39**, 2225 (2005).
[13] M. Petrakis, B. Psiloglou, P. Kassomenos, C. Cartalis, J. Air & Waste Management Association **53**, 1052 (2003).
[14] U. Platt, Phys. Chem. Chem. Phys. **1**, 5409 (1999).
[15] J. England, B. Lewis, and S. Gibson, Canadian J. Phys. **74**, 185 (1996).
[16] R. Ditchburn, and P. Young, J. Atmos. Terres. Phys. **24**, 127 (1962).
[17] E. Warburg, Ber. d. PreuB. Akad. D. Wissensch. 230 (1915).
[18] O. Wulf, Proceedings of the National Academy of America **14**, 356 (1928).
[19] W. Finkelnburg and W. Steiner, Zeitsehrift fur Physik. **79**, 69 (1932).
[20] M. R. Shardanand. Phys. Rev. **186**, 5 (1969).
[21] U. Platt, L. Marquard, T. Wagner, and D. Perner, Geophys. Res. Lett. **24**, 1759 (1997).
[22] K. Yoshino, J. R. Esmond, J. E. Murray, W. H. Parkinson, A. P. Thorne, R. C. M. Learner, and G. Cox, J. Chem. Phys. **103**, 1243 (1995).
[23] K. Yoshino, J. R. Esmond, W. H. Parkinson, A. P. Thorne, R. C. M. Learner, and G. Cox, J. Chem. Phys. **111**, 2960 (1999).
[24] K. Yoshino, J. R. Esmond, W. H. Parkinson, A. P. Thorne, R. C. M. Learner, and G. Cox, J. Chem. Phys. **112**, 9791 (2000).
[25] H. Axelsson, A. Eilard, A. Emanuelsson, B. Galle, H. Edner, P. Ragnarson, and H. Kloo, Appl. Spectr. **49**, 1254 (1995).
[26] B. Trost, Atmos. Environ. **31**, 3999 (1997)
[27] M. R. Shardanand. J. Quanti. Spect. Radia. Transfer. **18**, 525 (1977).
[28] G. D. Greenblatt, J. J. Orlando, J. B. Burkholder, and A. R. Ravishankara, J. Geophys. Res. **95**, 18577 (1990).
[29] J. Vattulainen, L. Wallenius, J. Stenberg, R. Hernberg, and V. Linna, Appl. Spectr. **57**, 1311 (1997).
[30] A. Savitzky and M. Golay, Anal. Chem. **36**, 1627 (1964).
[31] R. Volkamer, Ph.D. Dissertation, *Institut Fuer Umweltphysik*, University of Heidelberg, (1996).

DOI:10.1088/1674-0068/21/03/202-210